Chapter 12
Overview of Star-Forming Regions

Robert D. Mathieu

12.1 Introduction

The dynamical evolution of young star clusters and associations is an evolving interplay of the gravitational potential, as determined by the spatial distribution of gas and stars, and the motions of the gas and stars. Arguably, more investigation has been put into the content and structure of star-forming regions than any other aspect of star formation, far more than can be comprehensively presented here. Rather, the goal is to introduce a few nearby star-forming regions which are important for our discussion of dynamics. These regions are not characteristic in any systemic sense. Their significance derives from the extensive studies that have been applied to them over the years, and thus their role in laying the foundation for our understanding of star formation.

12.2 Taurus-Auriga

An appropriate place to start a discussion of the Taurus-Auriga[1] star-forming region is the spectacular photograph of the Taurus dark clouds taken by Barnard et al. (1927; see Fig. 12.1). The filamentary structure, the dense cores, even some of the young stellar objects are all evident in this image. At the time there was still discussion about whether these dark areas were intervening clouds or holes in the stellar distribution.

In Fig. 12.2 is shown a star count map and a *J*–*H* colour map based on the 2MASS all-sky survey data. Even in the near-infrared, the clouds remain defined by reduction in stellar surface density. Furthermore there is a close association of enhanced

[1] A detailed overview of the Taurus-Auriga star-forming region and its constituents can be found in Kenyon et al. (2008).

R.D. Mathieu (✉)
Department of Astronomy, University of Wisconsin, Madison, WI, USA
e-mail: mathieu@astro.wisc.edu

C.P.M. Bell et al. (eds.), *Dynamics of Young Star Clusters and Associations*,
Saas-Fee Advanced Course 42, DOI 10.1007/978-3-662-47290-3_12

Fig. 12.1 Photographic image of the Taurus dark clouds (Barnard et al. 1927)

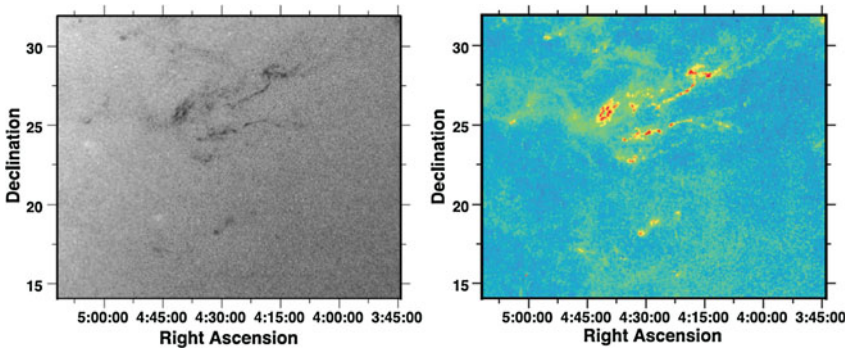

Fig. 12.2 Maps of near-infrared star counts (*left*) and J–H colours (*right*) in the Taurus-Auriga region, based on the 2MASS survey. Figure adapted from Kenyon et al. (2008)

reddening with low stellar surface density: evidently the Taurus-Auriga dark clouds are in fact dust clouds.

Figure 12.3 shows a CO $J = 1$-0 map of the Taurus-Auriga region, showing yet again the characteristic tilted U-shape distribution of the material in the region. The dust (see Fig. 12.2) and molecular gas are intimately associated. The total amount of molecular gas—the primary diffuse constituent—is about $10^4\,M_\odot$, so in fact the Taurus-Auriga clouds are a rather small star-forming region made important only by their proximity of 140 pc from the Sun.

Of particular importance is the evident clumpiness on smaller size scales (see Fig. 12.4). Sites of particular high extinction have long been known since they were

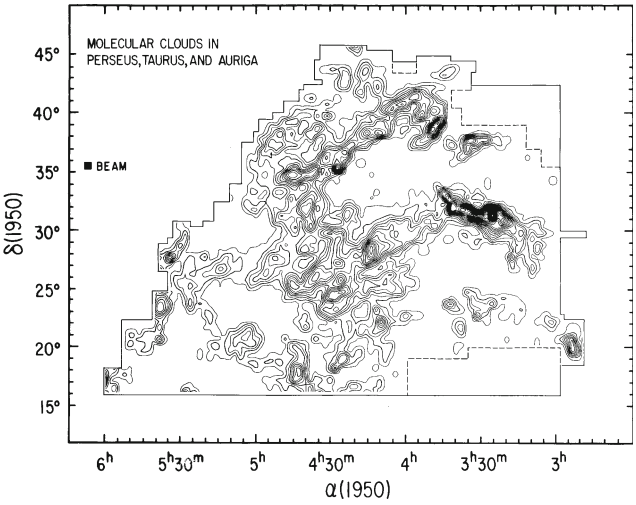

Fig. 12.3 Map of velocity-integrated CO emission. Figure from Ungerechts and Thaddeus (1987)

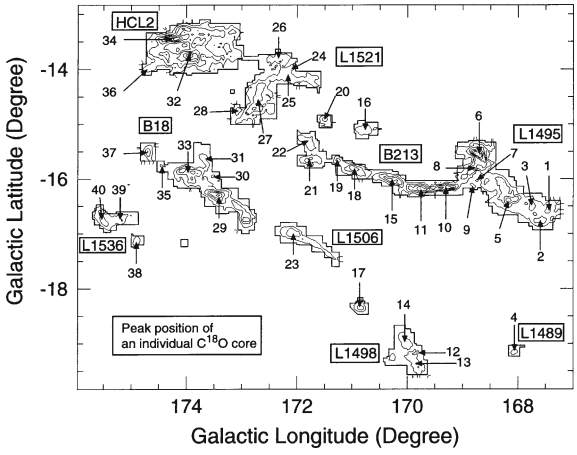

Fig. 12.4 Positions of cores in the Taurus region on a $C^{18}O$ integrated intensity map. Figure from Onishi et al. (1998)

catalogued by Barnard and later Lynds. These dense cores have been explored in depth over the last several decades, beginning with the pioneering studies by Myers and Benson with high-density molecular tracers ($>10^5$ cm^{-3}) that showed the cores to be sites of 1–10 $M_\odot$ of dense molecular gas roughly 0.1–1 pc in diameter.

With the launch of the IRAS satellite the close association of these dense molecular cores with low-mass star formation was evident in the correlation of infrared source positions with many of these cores. On the other hand, the X-ray survey missions such as ROSAT were effective at finding the chromospherically bright, often older, pre-main-sequence stars scattered throughout the region and not necessarily closely associated with the current distribution of gas and dust.

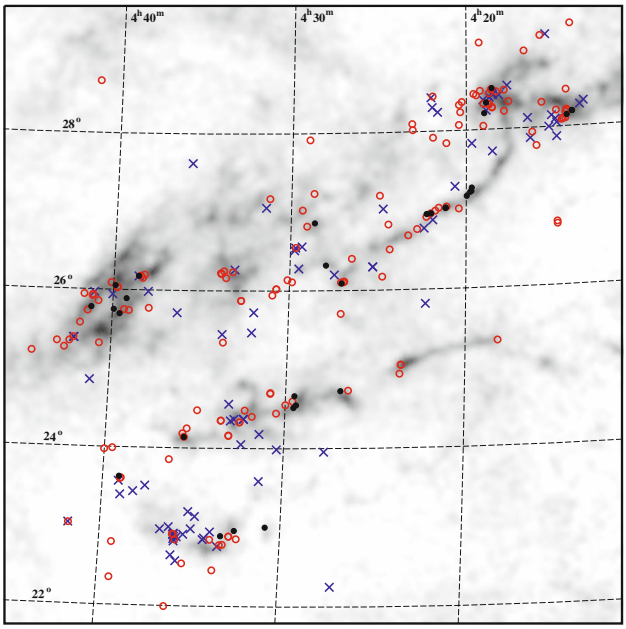

Fig. 12.5 Positions of Class 0/I (*black filled circles*), II (*red open circles*) and III (*blue crosses*) objects in the Taurus star-forming region superimposed on a greyscale extinction map. Figure from Luhman et al. (2010)

Figure 12.5 gives an overview of the young star distribution in the Taurus-Auriga clouds. Here Class 0/I objects have rising near- to far-infrared spectral energy distributions (deeply embedded protostars), Class II objects are T Tauri stars with active accretion discs ('classical T Tauri stars'), and Class III objects are pre-main-sequence stars suffering modest extinction with minimal or no circumstellar discs. The essential point of Fig. 12.5 is that there is an extremely tight correlation of the Class 0/I objects with the molecular gas distribution, while the Class III objects can be found both associated with gas or not. This evolving spatial distribution with evolutionary state (and, loosely, to astrophysical age) of young stars reflects the dissolution of this star-forming region.

The Class 0/I objects are highly spatially correlated, or clumped, with a mean separation of about 0.3 pc, which is on the order of dense core radii: the clumpiness in the molecular gas shows up in the stellar distributions, with surface densities of 20–30 pc^{-2} (e.g. Gomez et al. 1993).

Even so, these stellar surface densities are not sufficient to bind the groups. Indeed, other than the multiple star systems such as binaries and triples, there likely is no stellar structure in Taurus-Auriga that is itself bound. When the gas is dispersed—and how that happens is an open question given the lack of OB stars—the very loosely bound young stars of Taurus-Auriga will simply diffuse into the field star populations of the Milky Way.

12.3 Orion Molecular Cloud

The Orion Molecular Cloud (OMC) is the nearest giant molecular cloud, comprised of two sub-units, and is unremarkable in terms of its size or mass. Orion A is associated with the Orion Nebula Cluster (ONC) and the L1641 dark cloud. Orion B is associated with the Flame (NGC 2024) and Horsehead Nebulae (also NGC 2023, 2068, and 2071). Figure 12.6 shows the entirety of the cloud in 100 μm dust emission, and also places it in the Galactic context of other nearby star-forming regions. Detailed discussions of the stellar content as well as the gas and dust distributions in the region can be found within several chapters of the Handbook of Star Forming Regions Vol. II: The Southern Sky by Reipurth (2008).

Any discussion of the evolution of the several OB associations in the vicinity of the OMC must start with Adriaan Blaauw. Figure 12.7 is an optical image of the OMC region, identifying the associations studied by Blaauw in the early 1960s. For a sense of scale, at the top of the image is the λ Orionis association whose evolution was discussed in Chap. 11. Note that the size-scale of the clump of 10–12 OB stars at the core of the λ Ori region is comparable to the ONC and there are a comparable number of OB stars in the two regions. The essential difference is that the ONC is still associated with its natal gas, while in the older λ Ori region the natal gas has been dispersed, likely by a supernova.

Moving on to the classic OB associations of Blaauw, two of his essential findings were that the ages of the associations covered a range of ∼10 Myr and correlated inversely with their physical extent (as can be seen in Fig. 12.7). He further used proper motions to show that the so-called nuclear turn-off ages (from post-main-

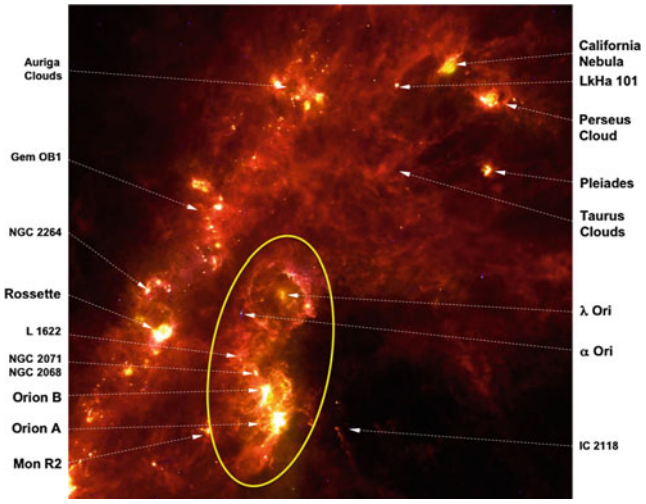

Fig. 12.6 100 μm map of the Galaxy in the direction of Orion. The Orion molecular cloud is shown within the oval. Figure adapted from Bally (2008)

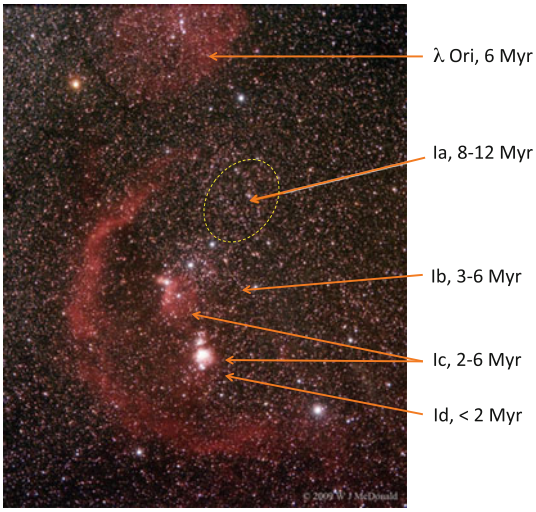

Fig. 12.7 Hα map of the OMC region, with classical OB associations and ages identified. Image courtesy of W.J. McDonald

sequence evolution of the most massive stars) correlated roughly with the dynamical (expansion) ages of the associations. Put simply, Orion was a laboratory to study the evolution and dissolution of OB associations.

Though Blaauw focused on the OBA stars, in fact low-mass star formation is also happening throughout the region, both within the OB associations and beyond. Of course this was also known by Blaauw and his contemporaries, given the rich population of T Tauri stars discovered through their variability and by Hα surveys. A modern near-infrared survey for variability is shown for Orion A in Fig. 12.8, showing the broad distribution of low-mass young stars along the north-south ridge. Given typical internal motions of $1\,\mathrm{km\,s^{-1}}$, the crossing time of even the denser Orion Nebula region exceeds the typical stellar ages of 1 Myr. Again, the structure of the gas tends to dictate the initial spatial distribution and dynamics of star-forming regions.

The highest density of near-infrared variables is associated with the ONC, the densest region of current star formation in Orion to which we will turn next. The essential point here from Fig. 12.8 is that star formation is a spatially continuous process throughout molecular clouds. We tend to classify and thereby segregate conceptually. But from the point of view of star formation, there is no clean boundary between the distributed star formation in L1641 and the rich cluster in the ONC (cf. Allen and Davis 2008). The distinction between T associations and OB associations is largely historical and observational. Every i.e. 'OB association' in the OMC also has an associated population of low-mass T Tauri stars.

Following the insight of Blaauw, let us now focus on a canonical case that illustrates the dynamical evolution of associations. The ONC (see Fig. 12.9; also known as the Trapezium Cluster) is the most massive, compact and youngest collection of young stars within the OMC. While an accounting depends on choice of boundary, the stellar population includes several thousand stars. The typical ages are 1–2 Myr, and others remain embedded along the line-of-sight. The IMF is log-normal

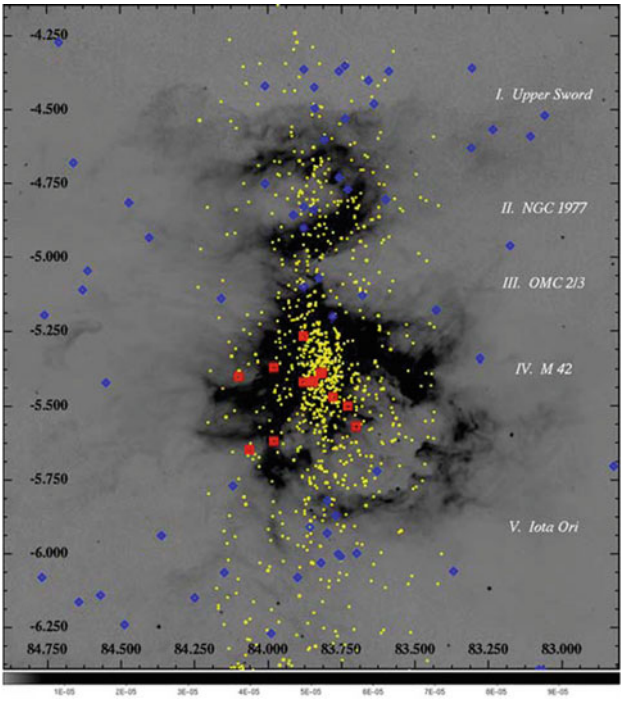

Fig. 12.8 The distribution of young stars toward Orion A. *Yellow circles* denote near-infrared variable stars, whereas the *blue diamonds* and *red squares* represent the OB members of the Orion OB1c and OB1d associations respectively. Note that the highest surface density of the *yellow circles* corresponds to the position of the Orion Nebula region. The reverse greyscale image is an MSX 8 μm image. Figure from Muench et al. (2008)

Fig. 12.9 The Orion Nebula Cluster at three wavelengths—optical (*left*), near-infrared (*middle*) and X-ray (*right*). Figures from Lada and Lada (2003) and Lada (2010)

(with some uncertainty at the very-lowest stellar masses; cf. Andersen et al. 2011; Da Rio et al. 2012), much like that derived from the field (Muench et al. 2002).

It is illustrative to consider the ONC as an open cluster as done by Hillenbrand and Hartmann (1998). King model fits yield a core radius of only 0.2 pc. Note that

the short crossing time of order 0.1 Myr supports the use of a dynamical equilibrium model, at least for the core. With 2200 stars within this radius, the core density becomes $2.1 \times 10^4\,M_\odot\,pc^{-3}$. The core radius is much smaller than typical for open clusters, and the core density much higher, by an order of magnitude.

However, the crossing time for stars in the halo of the cluster approaches or exceeds the ages of the stars. In fact, outside the core the cluster is clearly elongated in the north-south direction (see e.g. Fig. 1 in Hillenbrand and Hartmann 1998). Even if the gravitational potential is no longer dominated by the gas, most of these stars have not traversed the new potential; certainly much of the system has not completed violent relaxation (cf. the cold collapse scenario of Allison et al. 2010). Finally, the dynamical mass (i.e. derived from stellar motions) for the cluster is $4800\,M_\odot$ while the observed mass is $1800\,M_\odot$, which leaves open the possibility that the cluster may be unbound and expanding depending on the distribution of the gas mass and its contribution to the potential. With the possible exception of the core, the ONC will almost certainly evolve on dynamical timescales. Numerous authors have noticed that the ONC is mass segregated, at least for the most-massive stars (see e.g. Fig. 6 in Hillenbrand and Hartmann 1998). Whether this is the consequence of the star formation process or dynamical relaxation is a key question whose answer is not yet entirely clear. The two-body relaxation time for the core is of order 1 Myr, and dynamical friction on the most massive stars makes the equipartition time shorter still.

Perhaps the most interesting question for us is whether the ONC is destined to emerge as a bound open cluster or dissolve as the other OB subgroups in Orion. The comparison of the observed and dynamical masses suggests that the cluster is unbound. This seemingly straightforward conclusion is somewhat complicated by uncertainty about location of the gas. The Orion Nebula is well-known to be a blister on the front face of the OMC. We do not know whether the several thousand solar masses of gas along the line-of-sight are actually very near the cluster, dynamically associated with it and perhaps binding it together, or whether this material is well behind the cluster. In either case its tidal impact must also be considered in the cluster evolution. The answer to whether the cluster is bound or unbound may be 'yes' (as in a bit of both). As shown by N-body simulations (Lada et al. 1984; Kroupa and Boily 2002), after gas-loss a marginally bound system may leave behind a bound core surrounded by a dispersing halo. This may be the fate of the ONC. It certainly will not be a massive open cluster such as M67 or even the Pleiades, so we continue to search for examples of the progenitors of such systems. What is certain is that the current ONC will expand from its current state as a result of the loss of gas mass.

12.4 Young Embedded Clusters

With the advent of surveys with large format, sensitive, near-infrared images, it became evident that many and perhaps most young stars in giant molecular clouds

are formed in embedded clusters[2] containing dozens to several hundreds of stars with typical radii of <0.5 pc. Lada and Lada (2003) estimate about 200 embedded clusters within 2.5 kpc of the Sun, implying of order 10,000 such clusters in the Galaxy at the moment. Of course, determining membership for any given star in an infrared image is challenging. This challenge includes field stars in foreground projection, other stars forming in the molecular cloud but not associated with a particular spatial grouping, and background stars observed through patchy extinction. True members can be separated from field stars through signatures of youth, such as infrared excesses and chromospheric X-ray emission. These diagnostics do not distinguish other young stars in the molecular cloud, nor are such contaminants kinematically distinct.

Lada and Lada (2003) established commonly used dynamical criteria for embedded clusters. First, they require the stellar grouping to be stable against the tidal fields of the Galaxy and interstellar clouds. Lada (2010) notes that this requires of order 8–10 stars of 0.5 $M_\odot$ stars within a 1 pc radius. Second, they also require that, if bound, the two-body relaxation time not be shorter than the typical lifetime of open clusters of 100 Myr. This criterion requires 30–40 stars. Finally, the cluster should be partially or entirely embedded in its natal gas cloud. Importantly, there is no requirement that embedded clusters actually be bound by their stellar mass, but only that these criteria are satisfied should the cluster be bound. The mass spectrum of embedded

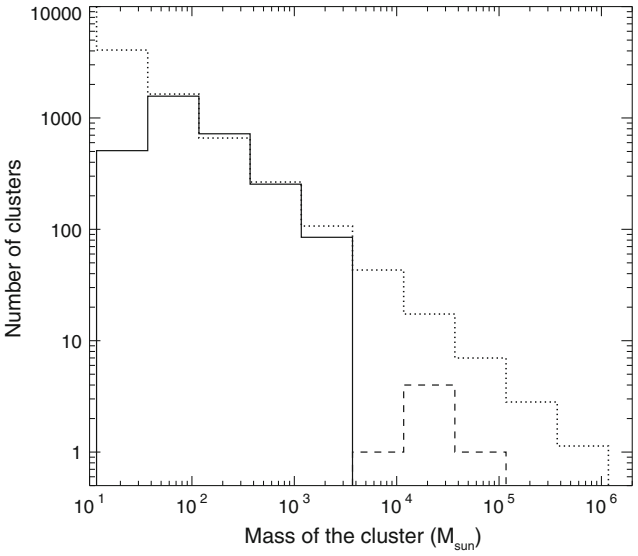

Fig. 12.10 The mass spectrum of embedded clusters for the Galaxy. The *solid line* shows the masses of clusters within 2.5 kpc (Lada and Lada 2003), while the *dashed line* shows massive embedded clusters from Ascenso (2008). The *dotted line* represents a spectral index of $\alpha = -1.7$. Figure from Lada (2010)

[2] A detailed review can be found in Lada and Lada (2003).

clusters is shown in Fig. 12.10. In the local Galaxy, the slope of the mass spectrum is reasonably represented as a power-law with spectral index α of between -1.7 and -2.0. Whether this distribution holds all the way to the most-massive young clusters, such as Westerlund 1, is not clear. If it does, more such clusters remain to be found. At the other extreme, the low-mass turnover in Fig. 12.10 seems to be real, but each of these groupings includes very few stars (e.g. Porras et al. 2003). In any case, many of the embedded clusters in the local Galaxy have very small masses. The spectral index of α with values of between -1.7 and -2.0 is interesting with respect to the question of in what environment is a star most likely to form. A slope of $\alpha = -2.0$ represents equal mass per decade: most stars forming in embedded clusters are just as likely to form in clusters with masses between 10 and 100 $M_\odot$ as in clusters between $10^{4-5} M_\odot$.

Wide-field infrared surveys of local molecular clouds indicate that most young stars are found in embedded clusters, perhaps as high as 70–90 % (see review in Lada and Lada 2003). This implies that this is the dominant mode of star formation in the Milky Way. In this context, it is interesting to compare the 'typical' star-forming region, in terms of total mass and central stellar density, to constraints on the birth site of our Solar System (Adams 2010). However there appears to be a continuum of embedded cluster properties, at least in stellar surface density, from the richest regions to the low-density aggregates (Meyer et al. 2008; Bressert et al. 2010). Clearly, the dynamics of young clusters and associations are intimately related (see e.g. Fig. 12.12) and their dissolution is a primary mechanism of populating the field. Because associations are thought to represent up to 90 % of the outcomes of star formation in the Galactic disc, this suggests that associations originate in embedded clusters.

Turning to the age distribution of young clusters, in a survey of young clusters Leisawitz et al. (1989) found that only clusters younger than 5 Myr were associated ($d < 25$ pc) with massive ($>2 \times 10^4 M_\odot$) molecular clouds. Leisawitz et al. (1989) conclude that during the 5 Myr after the formation of a cluster containing massive stars the interstellar environment changes dramatically, and by 10 Myr little remains of the natal giant molecular cloud. (This timescale is consistent with our detailed discussion of the λ Ori above; see Chap. 11). This provides an upper limit on the timescales for clusters to separate from their parent molecular clouds and perhaps molecular cloud lifetimes (if the onset of star formation is rapid once clouds form). The ages of the embedded clusters are more typically 1–3 Myr. Given that this is comparable to their internal age spreads, the definition of an age distribution for embedded clusters becomes a bit problematic. Somewhat better defined is their birth rate of 2–4 $\mathrm{kpc}^{-2}\,\mathrm{Myr}^{-1}$ (Lada and Lada 2003). This is ten times the formation rate derived from the population of currently bound open clusters.

Regarding the dynamics of young clusters, the survival rate is perhaps the most important issue. Figure 12.11 compares the expected age distribution given constant production and survival of embedded clusters to the observed distribution of cluster ages. By 10 Myr most embedded clusters have already disappeared, a timescale very similar to that for separation from their natal clouds. Evidently, the vast majority of

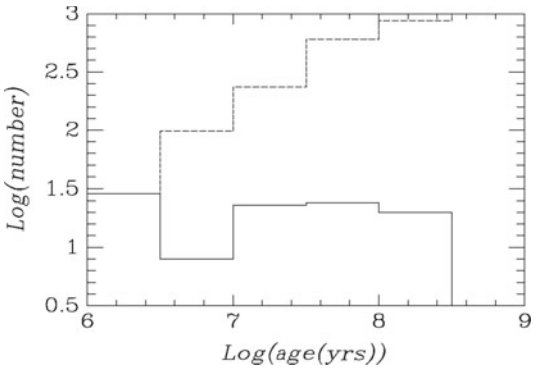

Fig. 12.11 Observed frequency distribution of ages for open and embedded clusters (*solid line*) compared with that predicted for a constant rate of cluster formation based on the embedded clusters (*dotted line*). By 3 Myr there is a discrepancy between number observed and predicted, suggesting that embedded clusters soon dissolve after leaving their natal molecular clouds. Figure from Lada and Lada (2003)

embedded star clusters do not survive emergence from their molecular clouds, and that they must dissolve in a way still to be determined.

At this point, a few remarks are in order. First, we tend to use the phrase 'bound' with regard to star-forming events carelessly: it is essential that we clearly define with the location, size-scale and the content of a region whose boundedness is under discussion. Location is important because given the irregular structure of star-forming regions the boundedness will vary. Size matters because even within regular structures cores may be bound while halos are unbound. Total content is critical because the role of gas in determining the gravitational potential within which young stars move can be dominant and transitory. A stellar system may be bound in the presence of gas and unbound with its loss.[3] Second, the internal structure of embedded clusters will play a role in the nature of their dissolution, and their boundedness. Lada and Lada (2003) suggest that there tend to be two qualitatively different structures. Of order 60 % tend to be compact, centrally condensed clusters, of which the Trapezium cluster is a more massive example. These can be fit with dynamical equilibrium models (e.g. King models). Others have very extended, irregular multiple peaks, such as the partially embedded cluster NGC 2264 (see Chap. 13, Fig. 13.4) to which fitting a dynamical equilibrium model would be truly nonsensical. In addition, most embedded clusters are elongated with aspect ratios as large as 2, much as found for the ONC (Allen et al. 2007). Figure 12.12 shows two regions—IC 348 and IC 2391—along with their dynamical times. Interestingly, the cluster structure does not correlate well with the dynamical (crossing) times. Despite an age of 20 dynamical times, the IC 2391 region is highly structured, looking more like an aggregate of subclusterings (each possibly in dynamical equilibrium). These regions may have

[3] It is worth reminding that gas is also subject to external pressure. As such, the boundedness of a gas cloud may not be a measure of the gravitational potential alone.

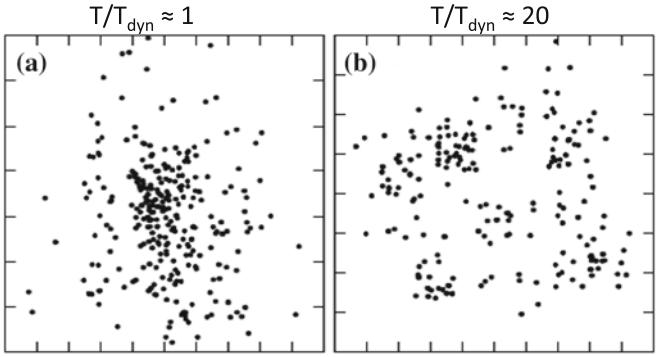

Fig. 12.12 Spatial distribution of low-mass stars in the regions of the IC 348 star-forming region (**a**) and the open cluster IC 2391 (**b**). Also shown are the ratios of cluster (stellar) ages to dynamical times. Figure adapted from Cartwright and Whitworth (2004)

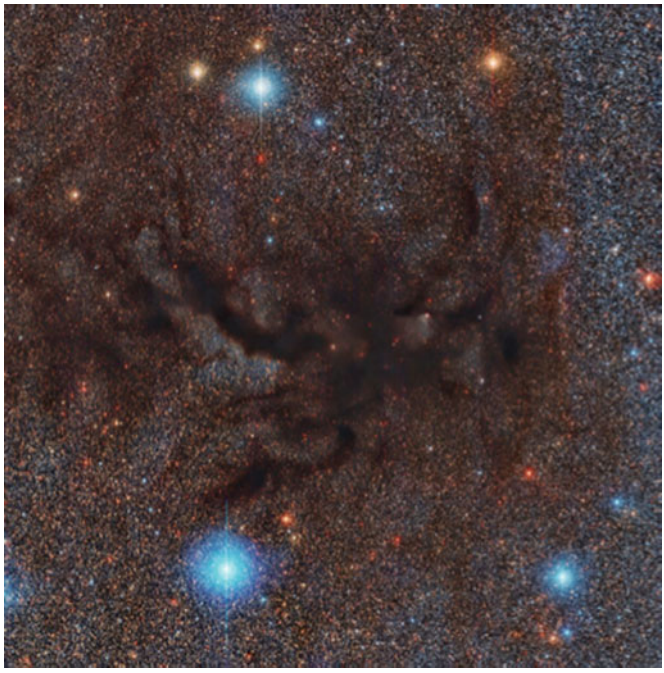

Fig. 12.13 Optical image of B59, a dense core at the intersection of an array of filaments and the site of an embedded cluster. Figure from Lada (2010)

experienced 'cold collapse' (a version of violent relaxation) described in detail in Chap. 6.

Finally, let me draw your attention to the beautiful image of the Barnard dark cloud B59 in Fig. 12.13. Myers (2009) argues that the filamentary structure of dark cloud

complexes play a major role in funnelling gas toward dense molecular cores, and earlier in this volume (see Clarke Chap. 6) we were shown several theoretical simulations suggesting the same. It is striking that where the filaments in Fig. 12.13 come together there is a small embedded cluster (e.g. Covey et al. 2010). This image is telling us vividly that we must let go of our simplifications ('the horse is a sphere'): there is a great deal of structure and complexity in these star-forming regions that may be crucial to the emergence of young clusters or associations.

References

Adams, F. C. 2010, ARA&A, 48, 47
Allen, L. E. & Davis, C. J. 2008, Handbook of Star Forming Regions, Volume I: The Northern Sky, ed. B. Reipurth, ASP Monograph Publications, 621
Allen, L., Megeath, S. T., Gutermuth, R., et al. 2007, Protostars and Planets V, ed. B. Reipurth, D. Jewitt & K. Keil, University of Arizona Press, 361
Allison, R. J., Goodwin, S. P., Parker, R. J., Portegies Zwart, S. F., & de Grijs, R. 2010, MNRAS, 407, 1098
Andersen, M., Meyer, M. R., Robberto, M., Bergeron, L. E., & Reid, N. 2011, A&A, 534, A10
Ascenso, J. 2008, PhD thesis, Centro de Astrofísica da Universidade do Porto
Bally, J. 2008, Handbook of Star Forming Regions, Volume I: The Northern Sky, ed. B. Reipurth, ASP Monograph Publications, 459
Barnard, E. E., Frost, E. B., & Calvert, M. R. 1927, A Photographic Atlas of Selected Regions of the Milky Way
Bressert, E., Bastian, N., Gutermuth, R. et al. 2010, MNRAS, 409, L54
Cartwright, A., & Whitworth, A. P. 2004, MNRAS, 348, 589
Covey, K. R., Lada, C. J., Román-Zúñiga, C., et al. 2010, ApJ, 722, 971
Da Rio, N., Robberto, M., Hillenbrand, L. A., Henning, T., & Stassun, K. G. 2012, ApJ, 748, 14
Hillenbrand, L. A., & Hartmann, L. W. 1998, ApJ, 492, 540
Kenyon, S. J., Gómez, M., & Whitney, B. A. 2008, Handbook of Star Forming Regions, Volume I: The Northern Sky, ed. B. Reipurth, ASP Monograph Publications, 405
Kroupa, P., & Boily, C. M. 2002, MNRAS, 336, 1188
Lada, C. J. 2010, Royal Society of London Philosophical Transactions Series A, 368, 713
Lada, C. J., & Lada, E. A. 2003, ARA&A, 41, 57
Lada, C. J., Margulis, M., & Dearborn, D. 1984, ApJ, 285, 141
Leisawitz, D., Bash, F. N., & Thaddeus, P. 1989, ApJS, 70, 731
Luhman, K. L., Allen, P. R., Espaillat, C., Hartmann, L., & Calvet, N. 2010, ApJS, 186, 111
Meyer, M. R., Flaherty, K., Levine, J. L., et al. 2008, Handbook of Star Forming Regions, Volume I: The Northern Sky, ed. B. Reipurth, ASP Monograph Publications, 662
Muench, A. A., Lada, E. A., Lada, C. J., & Alves, J. 2002, ApJ, 573, 366
Muench, A., Getman, K., Hillenbrand, L., & Preibisch, T. 2008, Handbook of Star Forming Regions, Volume I: The Northern Sky, ed. B. Reipurth, ASP Monograph Publications, 483
Myers, P. C. 2009, ApJ, 700, 1609
Onishi, T., Mizuno, A., Kawamura, A., Ogawa, H., & Fukui, Y. 1998, ApJ, 502, 296
Porras, A., Christopher, M., Allen, L., et al. 2003, AJ, 126, 1916
Reipurth, B. 2008, Handbook of Star Forming Regions, Volume II: The Southern Sky, ed. B. Reipurth, ASP Monograph Publications
Ungerechts, H., & Thaddeus, P. 1987, ApJS, 63, 645